arXiv:1109.5806v4 [hep-lat] 9 Aug 2012

Conformal fixed point of SU(3) gauge theory with 12 fundamental fermions

Tatsumi Aoyama,[1] Hiroaki Ikeda,[2] Masafumi Kurachi,[1] C.-J. David Lin,[3,4] Hideo Matsufuru,[5]
Kenji Ogawa,[3] Hiroshi Ohki,[1] Tetsuya Onogi,[6,*] Eigo Shintani,[7] and Takeshi Yamazaki[1]
[1]*Kobayashi-Maskawa Institute for the Origin of Particles and the Universe, Nagoya University, Nagoya 464-8602, Japan*
[2]*School of High Energy Accelerator Science, The Graduate University*
for Advanced Studies (Sokendai), Tsukuba 305-0801, Japan
[3]*Institute of Physics, National Chiao-Tung University, Hsinchu 300, Taiwan*
[4]*Division of Physics, National Centre for Theoretical Sciences, Hsinchu 300, Taiwan*
[5]*High Energy Accelerator Research Organisation (KEK), Tsukuba 305-0801, Japan*
[6]*Department of Physics, Osaka University, Toyonaka 560-0043, Japan*
[7]*RIKEN-BNL Research Centre, Brookhaven National Laboratory, Upton, NY 11973, USA*

We study the infrared properties of SU(3) gauge theory coupled to 12 massless Dirac fermions in the fundamental representation. The renormalized running coupling constant is calculated in the Twisted Polyakov loop scheme on the lattice. From the step-scaling analysis, we find that the infrared behavior of the theory is governed by a non-trivial fixed point.

PACS numbers: 11.10.Hi, 11.15.Ha, 11.25.Hf, 12.60.Nz, 11.30.Qc

In recent years, there have been growing interests in the phase structure of asymptotically-free gauge theories with various numbers of fermions (N_f) and their representations. In particular, it is important to gain knowledge of the critical N_f (denoted as $N_f^{\rm cr}$) where different infrared (IR) properties are distinguished. Below $N_f^{\rm cr}$, the theory is confining and chiral symmetry is broken, while above it there exists a non-trivial infrared fixed point (IRFP) which renders the theory conformal at low energy. The range $N_f^{\rm cr} \leq N_f \leq N_f^{\rm af}$ is called the conformal window, where $N_f^{\rm af}$ is the maximal N_f for the presence of asymptotic freedom.

In addition to its intrinsic field-theoretic interests, studies of (near) conformal nature of strongly coupled gauge theories are of great phenomenological significance. Such a theory is a candidate for the dynamical origin of the electroweak symmetry breaking. This has led to studies of conformal dynamics for various theories, using approaches such as the Schwinger-Dyson equation, the exact renormalization group, *etc.*. Among these methods, lattice gauge theory has been widely used as a reliable tool to perform first-principle computation of scheme-independent, universal quantities.

In this article we report results of a lattice study of SU(3) gauge theory coupled to 12 massless fermions in the fundamental representation [1–6]. There have been some recent lattice investigations in this theory, and the results have been controversial hitherto. In Ref. [2], the running coupling constant was computed in the Schrödinger functional (SF) scheme [7], and, within error, exhibited scale-independent behavior. Other works [3, 4] also showed the evidence of the conformal behavior in this theory. On the other hand, studies of the mass scaling behavior [5] and the spectrum of the Dirac operator [6] showed contradictive evidences.

The renormalized coupling constant itself is a scheme-dependent quantity. However, by identifying the relations among different renormalization schemes as coordinate transformations in the theory space, it can be demonstrated that the existence of a fixed point is scheme independent, except the case that the transformation is singular [8]. In view of this, the best method for the search of the IRFP is to look for zeros of the beta function. This leads us to focus on the ratio between the step-scaling function [9] and the input renormalized coupling constant. This ratio approaches one when the beta function approaches zero. To confirm the existence of an IRFP in an asymptotically-free gauge theory, it is important to demonstrate that the ratio is one at both ultraviolet (UV) and IR regimes, while being obviously different from this value in between.

We calculate the renormalized coupling constant in the Twisted Polyakov Loop (TPL) scheme [10] with the standard staggered dynamical fermions. This scheme has no $O(a)$ discretization error, which is a great advantage in taking the continuum limit. Another advantage is the absence of zero modes thanks to the twisted boundary condition, which enables us to perform simulation with massless fermions.

The TPL scheme was proposed in Ref. [10] for SU(2) gauge theory. Here we generalize it to the SU(3) case. To define the TPL scheme, we introduce twisted boundary condition for the link variables, $U_\mu(x)$, in x and y directions on the lattice,

$$U_\mu(x+\hat{\nu}L/a) = \Omega_\nu U_\mu(x)\Omega_\nu^\dagger, \quad (\nu = x, y) \qquad (1)$$

where L is the spatial extent and a is the lattice spacing. The twist matrix Ω_ν is chosen to satisfy $\Omega_\mu\Omega_\mu^\dagger = \mathbb{I}$, $(\Omega_\mu)^3 = \mathbb{I}$, $\mathrm{Tr}[\Omega_\mu] = 0$, and $\Omega_\mu\Omega_\nu = e^{i2\pi/3}\Omega_\nu\Omega_\mu$ for a given μ and $\nu(\neq \mu)$. In the present study, we choose to work with the twist matrix as in Ref. [11]. The gauge transformation of U_μ is defined as $U_\mu(r) \to \Lambda(r)U_\mu(r)\Lambda^\dagger(r+\hat{\mu})$, with $\Lambda(r)$ satisfying the relation $\Lambda(r+\hat{\nu}L/a) = \Omega_\nu\Lambda(r)\Omega_\nu^\dagger$ for the consistency with Eq.(1).

By requiring the gauge and translational invariance, the Polyakov loops in a twisted direction can be defined as

$$P_x(y,z,t) = \mathrm{Tr}\Big([\prod_j U_x(x=j,y,z,t)]\Omega_x e^{i2\pi y/3L}\Big). \quad (2)$$

Then the renormalized coupling in the TPL scheme is defined by taking the ratio of Polyakov loop correlators in the twisted (P_x) and the untwisted (P_z) directions:

$$g^2_{\mathrm{TPL}} = \frac{1}{k}\frac{\langle \sum_{y,z} P_x(y,z,L/2a)P_x(0,0,0)^\dagger\rangle}{\langle \sum_{x,y} P_z(x,y,L/2a)P_z(0,0,0)^\dagger\rangle}. \quad (3)$$

The leading discretization error is $O(a^2)$ in this scheme. At tree level, this ratio of the Polyakov loops is proportional to the square of the bare coupling. The proportionality factor k is obtained by analytically calculating the one-gluon-exchange diagram. In the case of SU(3) gauge group, the value of k with Wilson plaquette gauge action is

$$k^{\mathrm{latt.}}(a/L) \sim 0.03184 + 0.00453(a/L)^2 + O(a^4). \quad (4)$$

The discretization effects in k are of $O(a^2)$ instead of $O(a)$, as expected.

To include fermions in the fundamental representation with twisted boundary condition, we introduce the "smell" degrees of freedom [12] to avoid inconsistency with translational invariance. The smell quantum number is a copy of color, and its non-trivial effects only appear at the boundary. It is incorporated by identifying the fermion field as a $N_c \times N_s$ matrix, $\psi^a_\alpha(x)$, where a is the color index and α is the smell index. The twisted boundary condition for the fermion field is then imposed as

$$\psi^a_\alpha(x+\hat{\nu}L/a) = e^{i\pi/3}\Omega^{ab}_\nu \psi^b_\beta(\Omega_\nu)^\dagger_{\beta\alpha}, \quad (5)$$

for $\nu = x, y$ directions. The smell degrees of freedom introduced here can be considered as extra flavors. This means that the number of flavors we can study on the lattice is a multiple of $N_s(= N_c = 3)$. Furthermore, since we use staggered fermions in our simulation, we have four tastes for each flavor. This enables us to perform the computation with $N_f = 3 \times 4 = 12$ in SU(3) gauge theory with twisted boundary condition.

First, we discuss the vacuum structure and the existence of the true vacua in an SU(3) gauge theory involving massless fermions in the deconfining phase. The free energy of the pure-gauge sector contains 3^4-fold degenerate classical minima at $U_\mu = \exp(2\pi i\theta_\mu/3)\mathbb{I}$, where $\theta_\mu = 0, 1, 2$ for each space-time direction. We investigated the semi-classical free energy in $SU(3)$ gauge theory with $N_f = 12$ up to one loop level, and found that the vacuum energy is independent of $\theta_{1,2}$, and the vacua with both $\theta_{3,4}$ being 1 or 2 have the lowest free energy, indicating that those are the true vacua. For these "non-trivial vacua", all the classical link variables in z and t directions contain non-trivial phases $U_{3,4} \sim \exp(\pm 2\pi i/3L)$, giving rise to factors $\exp(\pm 2\pi i/3)$ in the Polyakov loops.

In this work, we generate gauge configurations around the true vacua where the vacuum expectation values of the Polyakov loops in untwisted directions have nontrivial phases. We observe that the vacuum stays having the nontrivial phases after thermalization and no transition to trivial vacuum occurs. On the other hand, there is transition between nontrivial vacua in the low β region. We monitored the value of the renormalized coupling during the transition and found that the contribution is negligible.

Our numerical simulation and analysis are conducted by the following guiding principles:

1. We generate data in a broad range of β, with intervals that g^2_{TPL} grows almost constantly in each interval. Thus the interval of β is large in high β region while small in the low β region. Each data have similar accuracy $(2-3\%)$.
2. We employ fit functions for β interpolation which reproduce the tree level result $g^2_{\mathrm{TPL}} \simeq g^2_0$ on each lattice size in extremely high β region.
3. We include only the data which ensure that systematic errors in all the interpolations and extrapolations are under control.

These guiding principles ensures the stability of our fit results under the change of fit functions. This is because the fit functions do not favor any special region of the data when we interpolate our data in β or extrapolate to in $(a/L)^2$ from the point 1, and the effect of statistical fluctuation in high β region where the growth of the coupling is small is reduced from the point 2, and the data $L/a = 4$ data, having the largest discretization effect, which was used in our previous report [13] is now dropped.

Our numerical simulation is performed in the following setup. The gauge configurations are generated by the Hybrid Monte Carlo algorithm, and we use the Wilson gauge and the staggered fermion actions. The simulations are carried out with lattice sizes $L/a = 6, 8, 10, 12, 16$ and 20 at around twenty β values ($\beta \equiv 6/g^2_0$ where g_0 is the bare coupling) in the range of $4.0 \leq \beta \leq 100$. To reduce statistical fluctuations, we generate 8,000–897,000 trajectories for each $(\beta, L/a)$ combination, measure the Polyakov loops at every trajectory and bin the data by taking the autocorrelation into account. The integrated autocorrelation time is about 400 trajectories on the largest lattices, while as small as 3–5 trajectories on the smallest lattices. Using the Jackknife method, typical statistical errors of correlators are $2-3\%$. The bootstrap analysis produces consistent results.

In Fig. 1, we show simulation results for the renormalized coupling as a function of $1/\beta$ for each L/a. For the

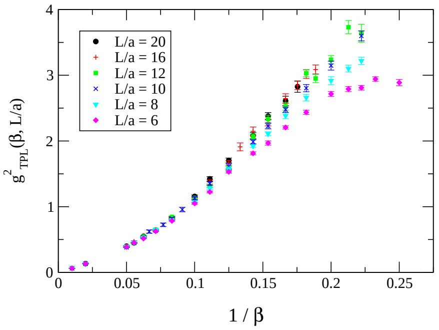

FIG. 1: TPL coupling for each β and L/a

purpose of β-interpolation, we use the following form of fitting function:

$$g^2_{\rm TPL}(\beta, a/L) = 6/\beta + \textstyle\sum_{i=1}^{N} C_i(a/L)/\beta^{i+1}, \tag{6}$$

where N is the degree of the polynomial and $C_i(a/L)$ are the fitting parameters. In order to obtain the best fit functions in which the χ^2/d.o.f. ~ 1, we take $N = 3 - 5$ depending on the lattice size.

To investigate the evolution of the renormalized running coupling, we employ step-scaling function with two lattice sizes scaled by a step-scaling parameter s. For each L/a in the set of smaller lattices, we find the value of β which produces a given value of the renormalized coupling, $u{=}g^2_{\rm TPL}(\beta, a/L)$. Then, we measure the renormalized gauge coupling at that β on the larger lattice, $\Sigma(u, a/L; s){=}g^2_{\rm TPL}(\beta, a/sL)|_{g^2_{\rm TPL}(\beta,a/L)=u}$. The step-scaling function, $\sigma(s, u)$, is obtained by taking the continuum limit of $\Sigma(u, a/L; s)$:

$$\sigma(s, u) = \lim_{a\to 0} \Sigma(u, a/L; s)|_{g^2_{\rm TPL}(\beta,a/L)=u}. \tag{7}$$

In this study, we take $s = 1.5$, and denote $\sigma(u) \equiv \sigma(s{=}1.5, u)$ in the rest of this letter for simplicity. The set of smaller lattice is taken to be $L/a = 6, 8, 10, 12$, and therefore, we need values of $g^2_{\rm TPL}$ for $L/a = 9, 12, 15, 18$ to take the continuum limit in Eq. (7). For $L/a = 9, 15$ and 18, we estimate values of $g^2_{\rm TPL}$ for a given β by the linear interpolation in $(a/L)^2$ with using the data on the lattices $L/a = \{8, 10\}$, $\{12, 16\}$ and $\{16, 20\}$, respectively. To estimate the systematic error of this interpolations, we also performed the linear interpolation in a/L, and found that the difference between a/L and $(a/L)^2$ interpolations is negligible.

In Fig. 2, we show an example of the continuum extrapolation for obtaining $\sigma(u)$ in the strong coupling region ($u = 2.054$). The procedure we use to derive the central value of $\sigma(u)$ is the linear extrapolation in $(a/L)^2$ with four points; $L/a = 6, 8, 10, 12 \to 9, 12, 15, 18$. Note that, in this example, though each lattice data $\Sigma(u, a/L; s = 1.5)$ is larger than u, in the continuum limit, $\sigma(u)$ is consistent with u. This indicates that it is very important to take the continuum limit carefully.

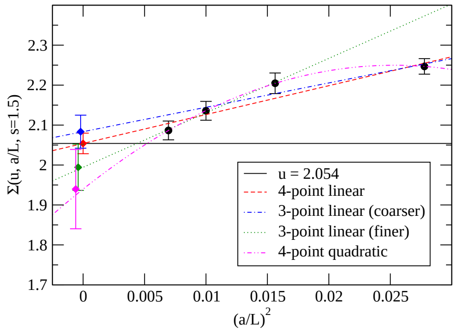

FIG. 2: Continuum extrapolation for the case of input coupling $u = 2.054$. Several kinds of extrapolation using all or various subsets of the data points are plotted.

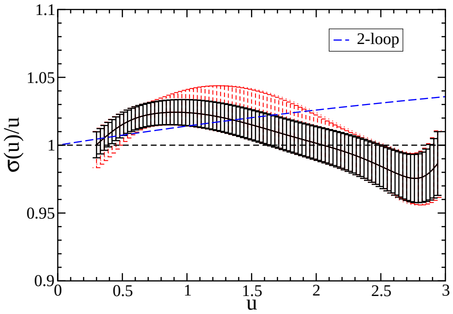

FIG. 3: The growth ratio $\sigma(u)/u$ as a function of u with statistical (solid) and total (dashed) errors. Two-loop perturbative value (dashed line) is also plotted for comparison.

We perform the step-scaling procedure explained above in a wide range of u. As mentioned in the beginning of this article, the growth rate $\sigma(u)/u$ is a suitable quantity for the search of the IRFP. This growth rate becomes one when there is a zero in the beta function. Figure 3 shows $\sigma(u)/u$ as a function of u with statistical (solid) and total (dashed) errors. The total error includes both the statistical and systematic errors. The statistical error is estimated by Jackknife method. We will explain our estimation of the systematic error in detail later. In the weak coupling regime, the result is consistent with perturbation theory. At $u = 2.05$, the central value of $\sigma(u)/u$ touches 1, demonstrating the existence of an IRFP. Though several data points are also shown for $u > 2.05$ in Fig. 3, we note that the continuum extrapolation cannot be performed reliably since the theory is not asymptotically free in this region.

We also study the running behavior of the renormalized coupling obtained from each 100 Jackknife ensembles. They all converge in the IR energy region, confirming the existence of the IRFP at

$$u^* = 2.05 \pm 0.47\,(\text{stat.})^{+0.20}_{-0.03}\,(\text{syst.}). \tag{8}$$

Here, the Jackknife error of the running coupling at IR is used as a statistical error. We will discuss our estimation of the systematic error in more detail later. The corresponding β value for each lattice size at $u^* = 2.05$ can be calculated from the β interpolation function in Eq. (6): $(\beta, L/a)$=(6.38,6), (6.65,8), (6.82,10), (6.96,12), (6.98,16), (7.02,18), (7.05,20). These are the parameter sets which reproduce conformal physics.

Since the value of the coupling constant at IRFP is scheme dependent, to compare with other schemes, we calculate the critical exponent of the beta function as a scheme-independent quantity. In the vicinity of the IRFP, the beta function can be approximated by $\beta(u) \simeq -\gamma(u^* - u)$, where γ is the critical exponent. We estimate γ from the slope of $\sigma(u)/u$ against u, and obtain $s^{-\gamma} = 0.95 \pm 0.03$. This leads to $\gamma = 0.14^{+0.08}_{-0.07}$, where the error is only statistical. Furthermore, if we use the different linear continuum extrapolation for $L/a = 6, 8, 10 \rightarrow 9, 12, 15$, we obtained $\gamma = 0.40 \pm 0.17$. This means our γ has a large systematic error. Still, the value we obtained here is consistent with both the perturbative results, $\gamma_{2-\mathrm{loop}} \sim 0.36$ and $\gamma^{(\overline{\mathrm{MS}})}_{4-\mathrm{loop}} \sim 0.28$ as estimated using 2-loop and 4-loop ($\overline{\mathrm{MS}}$ scheme), and the nonperturbative result in the SF scheme, $\gamma_{SF} = 0.13 \pm 0.03$ [2], within the systematic error. We remark that the value of γ is quite sensitive to the variation of the slope. Precise determination of the critical exponent is an important future problem to identify the interacting conformal fixed point. Another scheme-independent quantity which is interesting to observe is the mass anomalous dimension [3, 14] near the IRFP. We will report it in a forthcoming paper.

Here, we briefly mention the numerical stability of our results. For this purpose, we perform another step-scaling analysis based on $s = 2$ with $L/a = 6, 8, 10 \rightarrow 12, 16, 20$. The continuum limit is taken by linearly extrapolating these three points in $(a/L)^2$. We find that the running behavior in $s = 2$ step scaling is consistent with that in the case of $s = 1.5$, and the IRFP is found at $u^* = 2.26 \pm 0.64$ (stat.). This is consolidating the existence of the IRFP in this theory. We also derived the critical exponent of the beta function, and obtained $\gamma = 0.11 \pm 0.11$. This is also consistent with our main results with $s = 1.5$ shown in the previous paragraph.

Finally, we explain the systematic error in our analysis. There are two dominant sources of the systematic error. One is from the ambiguity of choosing the fit ansatz for the β-interpolation (Eq. (6)). The systematic error regarding this is estimated as follows: Once we find, in each L/a, an optimal number of N in Eq. (6) which gives a reasonable fit (which will be used for the derivation of central values), we change the number N to $N + 1$, and repeat the same fitting procedure. The difference between two fit results is adopted as the systematic ambiguity in each L/a. (We should mention here that the systematic ambiguity of β-interpolation for $L/a = 10$ is not included in our estimation of the systematic error since only $N = 4$ gives a reasonable fit.) The other dominant systematic error comes from the continuum extrapolation. In Fig. 2, we show the comparison of several types of continuum extrapolation. As the central value, we take the linear extrapolation in $(a/L)^2$ for $L/a = 6, 8, 10, 12 \rightarrow 9, 12, 15, 18$, and to estimate the systematic error in this procedure we estimate the differences between the central value and the linear extrapolation without the finest lattice $L/a = 12$. We estimate the total systematic error by adding these differences in two origins (five β interpolations and the continuum extrapolation) of systematic error in quadrature. Furthermore we compare the central value with the other linear continuum extrapolation without the coarsest lattice $L/a = 6$ and quadratic extrapolation with all the data at four L/a. All the values in the continuum limit agree within 1-σ statistical errors. For both of two analyses, the running region of u becomes narrower and the statistical error of u^* becomes much larger. Figure 3 shows the TPL renormalized coupling has a small systematic error in the strong coupling region, and we conclude that the existence of the IRFP is stable in this analysis.

To summarize, we have found solid evidence of the existence of an IRFP in SU(3) gauge theory with 12 massless Dirac fermions in the fundamental representation by using the TPL scheme. The procedure we presented here should be straightforwardly applied to studies of different gauge groups and fermion representations. It is also interesting to consider deformation of the theory at the UV scale with non-zero fermion mass or four-fermion interactions (see, e.g. [15]) in view of phenomenological applications.

We would like to thank G. Fleming, Y. Taniguchi, and N. Yamada for useful discussions. Numerical simulation was carried out on NEC SX-8 and Hitachi SR16000 at YITP, Kyoto University, NEC SX-8R at RCNP, Osaka University, and Hitachi SR11000 and IBM System Blue Gene Solution at KEK under its Large-Scale Simulation Program (No. 09/10-22 and 10-16), as well as on the GPU cluster at Taiwanese National Centre for High-performance Computing. We acknowledge Japan Lattice Data Grid for data transfer and storage. This work is supported in part by the Grant-in-Aid of the Ministry of Education (Nos. 20105002, 20105005, 21105508, and 23105708), and the National Science Council of Taiwan via grants 99-2112-M-009-004-MY3 and 099-2811-M-009-029.

---

[*] Electronic address: onogi@het.phys.sci.osaka-u.ac.jp

[1] Y. Iwasaki, K. Kanaya, S. Kaya, S. Sakai and T. Yoshie, Phys. Rev. D **69**, 014507 (2004).

[2] T. Appelquist, G. T. Fleming and E. T. Neil, Phys. Rev. Lett. **100**, 171607 (2008), [Erratum-ibid. **102**, 149902 (2009)], Phys. Rev. D **79**, 076010 (2009).

[3] T. Appelquist, G. T. Fleming, M. F. Lin, E. T. Neil and

D. A. Schaich, Phys. Rev. D **84**, 054501 (2011).

[4] A. Deuzeman, M. P. Lombardo, E. Pallante, Phys. Rev. **D82**, 074503 (2010).

[5] Z. Fodor, K. Holland, J. Kuti, D. Nogradi and C. Schroeder, Phys. Lett. B **703**, 348 (2011).

[6] Z. Fodor, K. Holland, J. Kuti, D. Nogradi and C. Schroeder, Phys. Lett. **B681**, 353 (2009).

[7] M. Luscher, R. Narayanan, P. Weisz and U. Wolff, Nucl. Phys. B **384**, 168 (1992).

[8] K. G. Wilson and J. B. Kogut, Phys. Rept. **12**, 75 (1974).

[9] M. Luscher, P. Weisz and U. Wolff, Nucl. Phys. B **359**, 221 (1991).

[10] G. M. de Divitiis, R. Frezzotti, M. Guagnelli and R. Petronzio, Nucl. Phys. B **422**, 382 (1994).

[11] H. D. Trottier, N. H. Shakespeare, G. P. Lepage and P. B. Mackenzie, Phys. Rev. D **65**, 094502 (2002).

[12] G. Parisi,Published in Cargese Summer Inst. 1983:0531

[13] E. Itou *et al.*, PoS **LATTICE2010** (2010) 054.

[14] S. Capitani, M. Luscher, R. Sommer and H. Wittig [ALPHA Collaboration], Nucl. Phys. B **544**, 669 (1999).

[15] Y. Kusafuka and H. Terao, Phys. Rev. D **84**, 125006 (2011).